Fraunhofer Institut
Techno- und
Wirtschaftsmathematik

On the relation between lattice variables and physical quantities in lattice Boltzmann simulations

Michael Junk
Dirk Kehrwald

13th July 2006

Kaiserslautern, Germany

Contents

1 Initial situation

In a domain $[0,T] \times \Omega$ with $\Omega \subset \mathbb{R}^d$, $d = 2, 3$, the incompressible Navier-Stokes equations take the form

$$\partial_\alpha u_\alpha = 0, \qquad \partial_t(\rho u_\alpha) + \partial_\beta(\rho u_\alpha u_\beta) + \partial_\alpha P = \mu \partial_\beta \partial_\beta u_\alpha + \rho a_\alpha \tag{1}$$

with

t : time in s

ρ : density in $\frac{\text{kg}}{\text{m}^3}$

u_α : components of the velocity vector in $\frac{\text{m}}{\text{s}}$

P : dynamic pressure in $\text{Pa} = \frac{\text{kg}}{\text{s}^2\text{m}}$

μ : hydrodynamic viscosity in $\text{Pa} \cdot \text{s} = \frac{\text{kg}}{\text{sm}}$

a_α : components of the acceleration vector due to a volume force in $\frac{\text{m}}{\text{s}^2}$

∂_t : time derivative

∂_α : space derivative in direction α.

Dividing the momentum equation in (1) by the constant density ρ, we obtain

$$\partial_\alpha u_\alpha = 0, \qquad \partial_t u_\alpha + \partial_\beta(u_\alpha u_\beta) + \partial_\alpha p = \nu \partial_\beta \partial_\beta u_\alpha + a_\alpha \tag{2}$$

with

$$p = \frac{P}{\rho} \text{ : kinematic pressure in } \frac{\text{m}^2}{\text{s}^2}$$

$$\nu = \frac{\mu}{\rho} \text{ : kinematic viscosity in } \frac{\text{m}^2}{\text{s}}.$$

2 Problem scale

While SI units are important to communicate the size of physical constants, their use to characterize specific problems is limited. For that purpose, it is preferable

to choose intrinsic or problem related units. Specifically, we use a characteristic length L^P [m], a characteristic time T^P [s], a typical velocity U^P [m/s] and characteristic acceleration A^P [m/s^2] and pressure P^P [m^2/s^2] to scale the Navier-Stokes equations (2). The relevant, non-dimensional quantities are defined by

$$\bar{x}_\alpha = \frac{x_\alpha}{L^P}, \quad \bar{u}_\alpha = \frac{u_\alpha}{U^P}, \quad \bar{t} = \frac{t}{T^P}, \quad \bar{p} = \frac{p}{P^P}, \quad \bar{a}_\alpha = \frac{a_\alpha}{A^P}, \tag{3a}$$

and therefore

$$\bar{\partial}_{\bar{t}} = T^P \partial_t, \quad \bar{\partial}_\alpha = L^P \partial_\alpha. \tag{3b}$$

Inserting those relations into (2), we obtain

$$\bar{\partial}_\alpha \bar{u}_\alpha = 0,$$
$$\frac{\left(U^P\right)^2}{T^P}\bar{\partial}_{\bar{t}}\bar{u}_\alpha + \frac{(U^P)^2}{L^P}\bar{\partial}_\beta(\bar{u}_\alpha\bar{u}_\beta) + \frac{P^P}{L^P}\bar{\partial}_\alpha\bar{p} - \frac{U^P\nu}{\left(L^P\right)^2}\bar{\partial}_\beta\bar{\partial}_\beta\bar{u}_\alpha = A^P\bar{a}_\alpha.$$

If we connect time, length and velocity scale according to $U^P = L^P/T^P$ and choose $P^P = (U^P)^2$ as typical pressure, we obtain

$$\bar{\partial}_\alpha\bar{u}_\alpha = 0, \qquad \bar{\partial}_{\bar{t}}\bar{u}_\alpha + \bar{\partial}_\beta(\bar{u}_\alpha\bar{u}_\beta) + \bar{\partial}_\alpha\bar{p} - \frac{1}{Re}\bar{\partial}_\beta\bar{\partial}_\beta\bar{u}_\alpha = \frac{1}{Fr}\bar{a}_\alpha$$

where Reynolds and Froude number are defined by

$$Re = \frac{L^P U^P}{\nu}, \quad Fr = \frac{\left(U^P\right)^2}{L^P A^P}.$$

3 Lattice scale

We consider a lattice Boltzmann algorithm of the form

$$f_i(t+\delta_t, \boldsymbol{x}+\delta_t\boldsymbol{c}_i) = f_i(t,\boldsymbol{x}) + J_i(\boldsymbol{f}(t,\boldsymbol{x})).$$

Choosing the typical length $L^{LB} = \delta_x$, the typical time $T^{LB} = \delta_t$ and the typical velocity $U^{LB} = c = \delta x/\delta t$, we obtain the scaled quantities

$$\hat{x}_\alpha = \frac{x_\alpha}{\delta_x}, \quad \hat{\boldsymbol{c}}_i = \frac{\boldsymbol{c}_i}{c}, \quad \hat{t} = \frac{t}{\delta_t},$$

which lead to the lattice Boltzmann equation in usual form

$$\hat{f}_i(\hat{t}+1, \hat{\boldsymbol{x}}+\hat{\boldsymbol{c}}_i) = \hat{f}_i(\hat{t}, \hat{\boldsymbol{x}}) + J_i(\hat{\boldsymbol{f}}(\hat{t}, \hat{\boldsymbol{x}})),$$

where

$$\hat{\rho} = \sum_i \hat{f}_i, \quad \hat{p} = c_s^2 \left(\hat{\rho} - 1\right), \quad \hat{\rho}\hat{\boldsymbol{u}} = \sum_i \hat{\boldsymbol{c}}_i f_i.$$

If the same scaling is used for the Navier-Stokes equation, we recover the form

$$\hat{\partial}_\alpha \hat{u}_\alpha = 0, \qquad \hat{\partial}_{\hat{t}} \hat{u}_\alpha + \hat{\partial}_\beta(\hat{u}_\alpha \hat{u}_\beta) + \hat{\partial}_\alpha \hat{p} - \frac{1}{Re^{LB}} \hat{\partial}_\beta \hat{\partial}_\beta \hat{u}_\alpha = \frac{1}{Fr^{LB}} \bar{a}_\alpha$$

with

$$Re^{LB} = \frac{c\delta_x}{\nu}, \qquad Fr^{LB} = \frac{c^2}{\delta_x A^P}.$$

4 Asymptotic analysis scale

Using asymptotic analysis the relation between the lattice Boltzmann algorithm and the Navier-Stokes equation can be clarified. To simplify the computation, a scaling which is characteristic for both the flow problem and the algorithm is used. Specifically, the length scale is $L^A = L^P$, the velocity scale is $U^A = c\delta_x / L^P$ with related time scale $T^A = L^A / U^A$. This choice leads to a relation between scaled space and time steps $\Delta x = \delta_x / L^A$ and $\Delta t = \delta_t / T^A$

$$\Delta t = \frac{\delta_t}{T^A} = \frac{\delta_x U^A}{c L^A} = \frac{\delta_x^2 c}{c (L^A)^2} = \Delta x^2.$$

If the Navier-Stokes equations are non-dimensionalized with respect to the asymptotic analysis scale, they have the form

$$\tilde{\partial}_\alpha \tilde{u}_\alpha = 0, \qquad \tilde{\partial}_{\tilde{t}} \tilde{u}_\alpha + \tilde{\partial}_\beta(\tilde{u}_\alpha \tilde{u}_\beta) + \tilde{\partial}_\alpha \tilde{p} - \frac{1}{Re^A} \tilde{\partial}_\beta \tilde{\partial}_\beta \tilde{u}_\alpha = \frac{1}{Fr^A} \bar{a}_\alpha \tag{4}$$

where Reynolds and Froude number are defined by

$$Re^A = \frac{L^A U^A}{\nu}, \qquad Fr^A = \frac{\left(U^A\right)^2}{L^A A^P}.$$

We remark that due to the definition of U^A, we have

$$Re^A = Re^{LB}, \qquad Fr^A = Fr^{LB}\Delta x^3$$

The relation to the parameters in the problem scale is given by

$$Re^A = Re\frac{\Delta x}{Ma}, \qquad Fr^A = Fr\left(\frac{\Delta x}{Ma}\right)^2, \qquad Ma = \frac{U^P}{c}$$

Results of the asymptotic analysis (for example in [1]) can now easily be translated to the other relevant scales.

5 Using the asymptotic analysis

In [1] it is reported that for $\tilde{t} = n\Delta t$ and $\tilde{x} = \boldsymbol{j}\Delta x$, the algorithm

$$\tilde{f}_i(n+1, \boldsymbol{j} + \hat{\boldsymbol{c}}_i) = \tilde{f}_i(n, \boldsymbol{j}) + J_i(\tilde{\boldsymbol{f}}(n, \boldsymbol{j})) + \Delta x^3 c_s^{-2} f_i^* \hat{\boldsymbol{c}}_i \cdot \tilde{\boldsymbol{G}}(n, \boldsymbol{j})$$

is consistent to the Navier-Stokes problem

$$\tilde{\partial}_\alpha \tilde{u}_\alpha = 0, \qquad \tilde{\partial}_{\tilde{t}} \tilde{u}_\alpha + \tilde{\partial}_\beta(\tilde{u}_\alpha \tilde{u}_\beta) + \tilde{\partial}_\alpha \tilde{p} = \left(\psi - \frac{1}{2}\kappa c_s^2\right)\tilde{\partial}_\beta \tilde{\partial}_\beta \tilde{u}_\alpha + \tilde{G}_\alpha \tag{5}$$

provided the collision operator is of the form

$$J_i(\boldsymbol{f}) = A(\boldsymbol{f}^{eq}(\boldsymbol{f}) - \boldsymbol{f})$$

where the collision matrix A has eigenvectors $\Lambda_i^{\alpha\beta} = c_{i\alpha}c_{i\beta} - \frac{1}{d}c_{i\gamma}c_{i\gamma}\delta_{\alpha\beta}$ with common eigenvalue $\lambda = \kappa c_s^2/\psi$. The flow variables $(\tilde{\boldsymbol{u}}, \tilde{p})$ are connected to $\tilde{\boldsymbol{f}}$ via

$$\tilde{\rho} = \sum_i \tilde{f}_i, \quad \tilde{p}\Delta x^2 = c_s^2\left(\tilde{\rho} - 1\right), \quad \tilde{\boldsymbol{u}}\Delta x = \sum_i \hat{\boldsymbol{c}}_i \tilde{f}_i.$$

Due to $L^A = L^P$ and $Re^A = Re\Delta x/Ma$ we have $U^A = U^P\Delta x/Ma$, and therefore

$$\bar{x}_\alpha = \frac{x_\alpha}{L^P} = \frac{x_\alpha}{L^A} = \tilde{x}_\alpha = \boldsymbol{j}\Delta x, \tag{6a}$$

$$\bar{t} = \frac{U^P}{L^P}t = \frac{Ma}{\Delta x}\frac{U^A}{L^A}t = \frac{Ma}{\Delta x}\tilde{t} = \frac{Ma}{\Delta x}n\Delta t, \tag{6b}$$

$$\bar{u}_\alpha = \frac{u_\alpha}{U^P} = \frac{\Delta x}{Ma}\frac{u_\alpha}{U^A} = \frac{\Delta x}{Ma}\tilde{u}_\alpha, \tag{6c}$$

$$\bar{p} = \frac{p}{(U^P)^2} = \frac{\Delta x^2}{Ma^2}\frac{p}{(U^A)^2} = \frac{\Delta x^2}{Ma^2}\tilde{p} \tag{6d}$$

In order to match the required viscosity parameter $1/Re^A$ in (4), we need

$$\frac{1}{Re^A} = \psi - \frac{1}{2}\kappa c_s^2 = \kappa c_s^2 \left(\frac{1}{\lambda} - \frac{1}{2}\right) = \tilde{\nu}.$$

Using the relation between Re^A and Re, we come to the conclusion

$$\tilde{\nu} = \frac{1}{Re^{LB}} = \frac{1}{Re}\frac{Ma}{\Delta x}$$

Comparing (5) and (4), we see that G_α has to be equal to $\bar{a}_\alpha/Fr^A$ to make sure that the lattice Boltzmann algorithm approximates the correct problem. The force term in the algorithm thus needs to be of the form

$$\frac{1}{Fr^A}\Delta x^3 c_s^{-2} f_i^* \boldsymbol{c}_i \cdot \tilde{\boldsymbol{a}} = \frac{1}{Fr^{LB}} c_s^{-2} f_i^* \boldsymbol{c}_i \cdot \tilde{\boldsymbol{a}} = \frac{1}{Fr} Ma^2 \Delta x c_s^{-2} f_i^* \boldsymbol{c}_i \cdot \tilde{\boldsymbol{a}}.$$

Note that the function $\tilde{\boldsymbol{a}}$ differs from $\bar{\boldsymbol{a}}$ in (3) only in the time argument which is scaled with respect to T^A instead of T^P.

In summary, the lattice Boltzmann algorithm

$$\tilde{f}_i(n+1, \boldsymbol{j} + \hat{\boldsymbol{c}}_i) = \tilde{f}_i(n, \boldsymbol{j}) + J_i(\tilde{\boldsymbol{f}}(n, \boldsymbol{j})) + \frac{Ma^2}{Fr}\frac{\Delta x}{c_s^2} f_i^* \hat{\boldsymbol{c}}_i \cdot \bar{\boldsymbol{a}} \tag{7a}$$

is consistent to the Navier-Stokes problem

$$\tilde{\partial}_\alpha \tilde{u}_\alpha = 0, \qquad \tilde{\partial}_{\tilde{t}} \tilde{u}_\alpha + \tilde{\partial}_\beta(\tilde{u}_\alpha \tilde{u}_\beta) + \tilde{\partial}_\alpha \tilde{p} = \frac{Ma}{\Delta x}\frac{1}{Re}\tilde{\partial}_\beta \tilde{\partial}_\beta \tilde{u}_\alpha + \frac{Ma^2}{\Delta x^2}\frac{\bar{a}_\alpha}{Fr}. \tag{7b}$$

Keeping in mind that $Ma = \mathcal{O}(\Delta x)$ is required for consistency to the incompressible Navier-Stokes equations [2] we choose an appropriate $\varphi > 0$ such that $Ma = \varphi \Delta x$, so we can rewrite equations (7) in the form

$$\tilde{f}_i(n+1, \boldsymbol{j} + \hat{\boldsymbol{c}}_i) = \tilde{f}_i(n, \boldsymbol{j}) + J_i(\tilde{\boldsymbol{f}}(n, \boldsymbol{j})) + \frac{\varphi^2}{Fr}\frac{\Delta x^3}{c_s^2} f_i^* \hat{\boldsymbol{c}}_i \cdot \bar{\boldsymbol{a}} \tag{8a}$$

respectively

$$\tilde{\partial}_\alpha \tilde{u}_\alpha = 0, \qquad \tilde{\partial}_{\tilde{t}} \tilde{u}_\alpha + \tilde{\partial}_\beta(\tilde{u}_\alpha \tilde{u}_\beta) + \tilde{\partial}_\alpha \tilde{p} = \frac{\varphi}{Re}\tilde{\partial}_\beta \tilde{\partial}_\beta \tilde{u}_\alpha + \frac{\varphi^2}{Fr}\bar{a}_\alpha, \tag{8b}$$

and (6) reduces to

$$\bar{x}_\alpha = \tilde{x}_\alpha = \boldsymbol{j}\Delta x, \qquad \bar{t} = \varphi \tilde{t} = n\varphi \Delta t, \qquad \bar{u}_\alpha = \frac{\tilde{u}}{\varphi}, \qquad \bar{p} = \frac{\tilde{p}}{\varphi^2}.$$

6 Comparison to the previous approach

Previously, a direct approach to express stationary Navier-Stokes equations (2) in lattice units was used at Fraunhofer ITWM. This approach was based on the simulation parameters $\tilde{\nu}$ and $\breve{a}_\alpha$ as well as the characteristic quantities

$$L^{LB} = \delta x, \qquad U^{old} = \frac{\nu}{\tilde{\nu}\delta x}, \qquad T^{old} = \frac{\tilde{\nu}\delta x^2}{\nu}.$$

This approach leads to the scaled Navier-Stokes problem

$$\check{\partial}_\alpha \breve{u}_\alpha = 0, \qquad \check{\partial}_t \breve{u}_\alpha + \check{\partial}_\beta(\breve{u}_\alpha \breve{u}_\beta) + \check{\partial}_\alpha \breve{p} = \tilde{\nu}\check{\partial}_\beta\check{\partial}_\beta \breve{u}_\alpha + \breve{a}_\alpha$$

with

$$\breve{x}_\alpha = \frac{x}{L^{LB}}, \quad \check{t} = \frac{t}{T^{old}}, \quad \breve{u}_\alpha = \frac{u_\alpha}{U^{old}}, \quad \breve{p} = \frac{p}{(U^{old})^2}, \quad \breve{a}_\alpha = \frac{\delta x}{(U^{old})^2} a_\alpha$$

and the lattice Boltzmann algorithm

$$\check{f}_i(\check{t} + \delta t, \breve{\boldsymbol{x}} + \hat{\boldsymbol{c}}_i \delta x) = \check{f}_i(\check{t}, \breve{\boldsymbol{x}}) + J_i\left(\check{\boldsymbol{f}}\left(\check{t}, \breve{\boldsymbol{x}}\right)\right) + f_i^* \frac{\hat{\boldsymbol{c}}_i \cdot \breve{\boldsymbol{a}}}{c_s^2}.$$

Comparing this model to equations (8), we find that the old model corresponds to the special case

$$\varphi = \frac{U^P L^P}{U^{old}\delta x}, \qquad L^P = L^{LB} = \delta x$$

in (8) and, therefore, to the lattice scale model discussed in Section 3.

7 A specific example

We consider a flow in an infinite vertical channel filled with turpentine under the action of constant gravity. The width of the channel is 1 mm, the initial velocity is zero, the hydrodynamic viscosity is $\mu = 1490$ μPa s, the density is $\rho = 0.86$ g/cm^3 and the acceleration is $-(0, g)$ where $g = 9.81$ m/s^2.

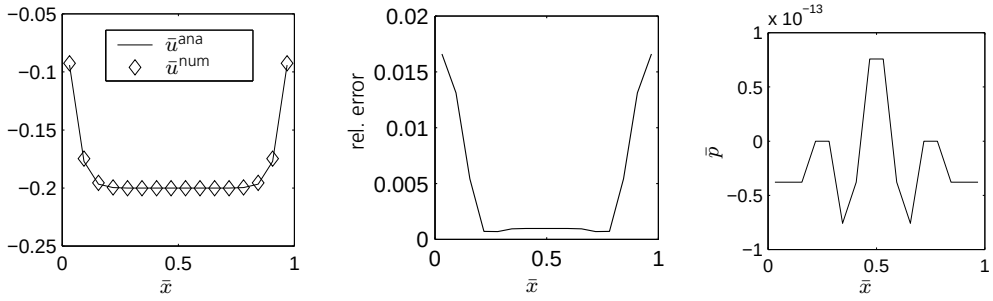

Figure 1 Numerical velocity $\bar{u}^{\text{num}}$ and analytical velocity $\bar{u}^{\text{ana}}$ (left), relative error $\left\|\bar{\boldsymbol{u}} - \boldsymbol{u}^{\overline{\text{num}}}\right\|_2 / \|\bar{\boldsymbol{u}}\|_2$ (middle), as well as numerical pressure $\bar{p}$ (right) for $\bar{t} = 0.2$, $\varphi = 0.5$, and $\Delta x = 1/16$

As problem scales, we take $L^P = 1$ mm and $A^P = g$. The velocity and time scales are then derived (for example) from the acceleration and length scale $T^P = \sqrt{L^P/A^P} \approx 0.0101$ s and $U^P = L^P/T^P = \sqrt{A^P L^P} \approx 0.099$ m/s. As Reynolds and Froude number, we find

$$Re = \frac{\rho L^P U^P}{\mu} \approx 57.17, \qquad Fr = 1.$$

Since the force term is constant in space and time, we have $\bar{\boldsymbol{a}} = \tilde{\boldsymbol{a}} = -(0,1)$. The solution of the scaled Navier-Stokes problem has the form

$$\bar{\boldsymbol{u}}\left(\bar{t}, \bar{\boldsymbol{x}}\right) = \left(0, \bar{v}\left(\bar{t}, \bar{x}\right)\right), \qquad \bar{p}(\bar{t}, \bar{\boldsymbol{x}}) = 0.$$

where

$$\bar{v}\left(\bar{t}, \bar{x}\right) = \frac{Re}{Fr} \sum_{n=0}^{\infty} \left(\exp\left(-\frac{Fr}{Re} \bar{t} \lambda_n^2 \right) - 1 \right) \frac{4}{\lambda_n^3} \sin\left(\lambda_n \bar{x}\right), \qquad \lambda_n = (2n+1)\pi$$

with limit value

$$\lim_{\bar{t} \to \infty} v(\bar{t}, \bar{x}) = \frac{1}{2} \frac{Re}{Fr} \bar{x}(\bar{x} - 1).$$

In order to run a lattice Boltzmann simulation, we choose a discretization parameter $\Delta x = \delta_x / L^P$ and a suitable value for $Ma = U^P/c$ which should not be too far from Δx to ensure proper convergence to the Navier-Stokes equations. Setting $Ma = \varphi \Delta x$, the relaxation time parameter $\tilde{\nu}$ has to be set to $\tilde{\nu} = \varphi / Re$ and the lattice Boltzmann algorithm reads

$$\hat{f}_i(n+1, \boldsymbol{j} + \boldsymbol{c}_i) = \hat{f}_i(n, \boldsymbol{j}) + J_i(\hat{\boldsymbol{f}}(n, \boldsymbol{j})) - \varphi^2 \Delta x^3 c_s^{-2} f_i^* \boldsymbol{c}_{iy}$$

A comparison of numerical and exact solutions (in the problem scale) for $\bar{t} \in \{0.2, 0.4, 0.6, 0.8, 1.0, 3.0\}$, $\varphi \in \{0.5, 8.0\}$, and $\Delta x \in \{1/16, 1/32\}$ is given in Figures 1 to 24.

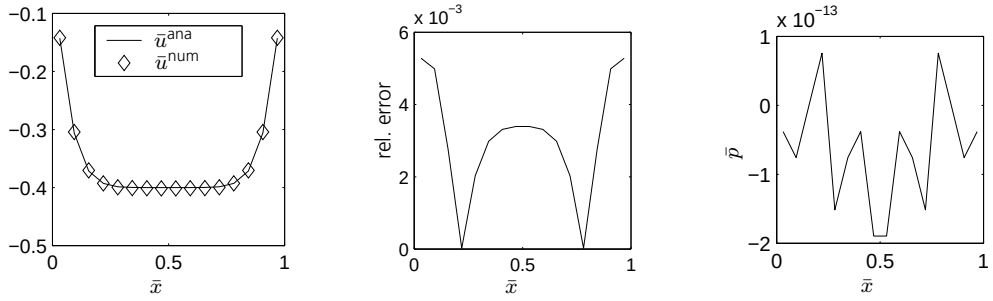

Figure 2 Numerical velocity $\bar{u}^{\text{num}}$ and analytical velocity $\bar{u}^{\text{ana}}$ (left), relative error $\left\|\bar{\boldsymbol{u}} - \boldsymbol{u}^{\bar{\text{num}}}\right\|_2 / \|\bar{\boldsymbol{u}}\|_2$ (middle), as well as numerical pressure $\bar{p}$ (right) for $\bar{t} = 0.4$, $\varphi = 0.5$, and $\Delta x = 1/16$

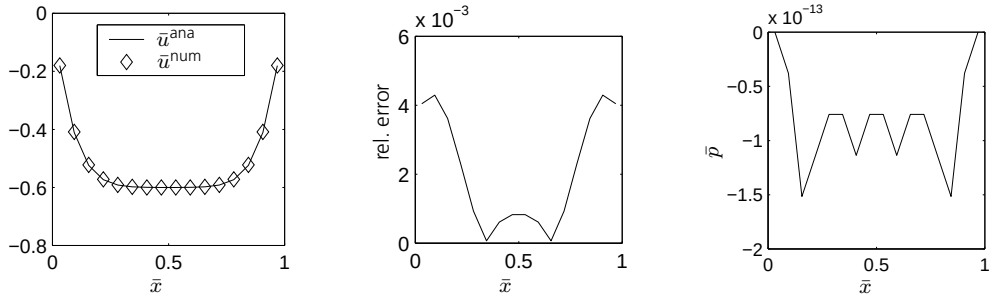

Figure 3 Numerical velocity $\bar{u}^{\text{num}}$ and analytical velocity $\bar{u}^{\text{ana}}$ (left), relative error $\left\|\bar{\boldsymbol{u}} - \boldsymbol{u}^{\bar{\text{num}}}\right\|_2 / \|\bar{\boldsymbol{u}}\|_2$ (middle), as well as numerical pressure $\bar{p}$ (right) for $\bar{t} = 0.6$, $\varphi = 0.5$, and $\Delta x = 1/16$

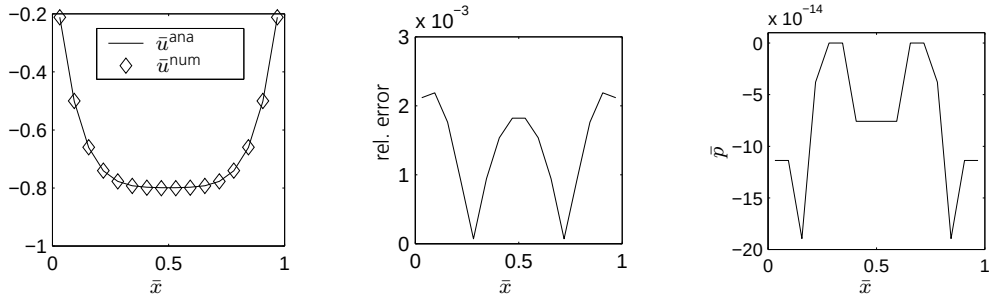

Figure 4 Numerical velocity $\bar{u}^{\text{num}}$ and analytical velocity $\bar{u}^{\text{ana}}$ (left), relative error $\left\|\bar{\boldsymbol{u}} - \boldsymbol{u}^{\bar{\text{num}}}\right\|_2 / \|\bar{\boldsymbol{u}}\|_2$ (middle), as well as numerical pressure $\bar{p}$ (right) for $\bar{t} = 0.8$, $\varphi = 0.5$, and $\Delta x = 1/16$

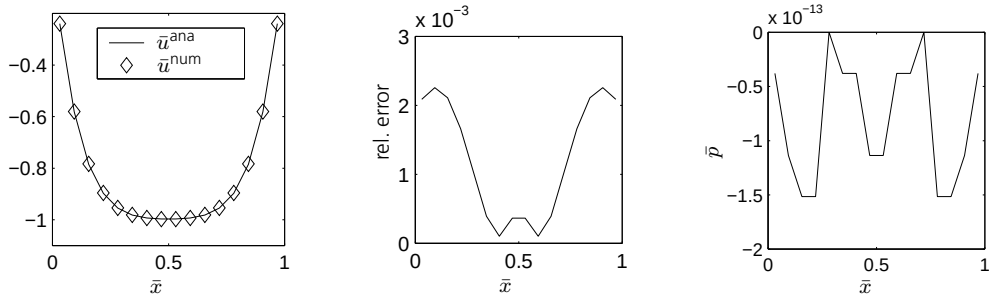

Figure 5 Numerical velocity $\bar{u}^{\text{num}}$ and analytical velocity $\bar{u}^{\text{ana}}$ (left), relative error $\left\|\bar{\boldsymbol{u}} - \boldsymbol{u}^{\bar{\text{num}}}\right\|_2 / \|\bar{\boldsymbol{u}}\|_2$ (middle), as well as numerical pressure $\bar{p}$ (right) for $\bar{t} = 1.0$, $\varphi = 0.5$, and $\Delta x = 1/16$

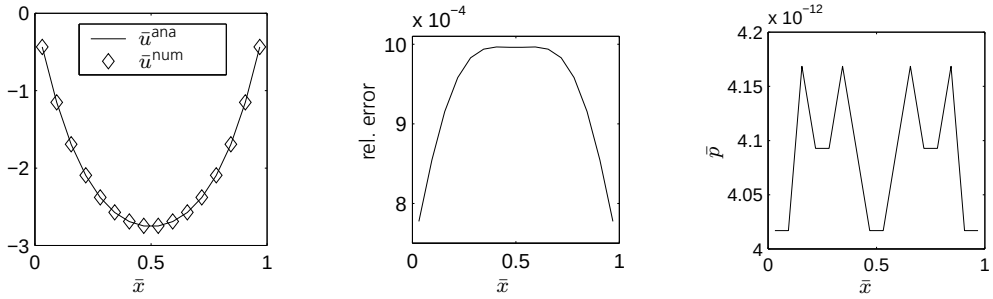

Figure 6 Numerical velocity $\bar{u}^{\text{num}}$ and analytical velocity $\bar{u}^{\text{ana}}$ (left), relative error $\left\|\bar{\boldsymbol{u}} - \boldsymbol{u}^{\bar{\text{num}}}\right\|_2 / \|\bar{\boldsymbol{u}}\|_2$ (middle), as well as numerical pressure $\bar{p}$ (right) for $\bar{t} = 3.0$, $\varphi = 0.5$, and $\Delta x = 1/16$

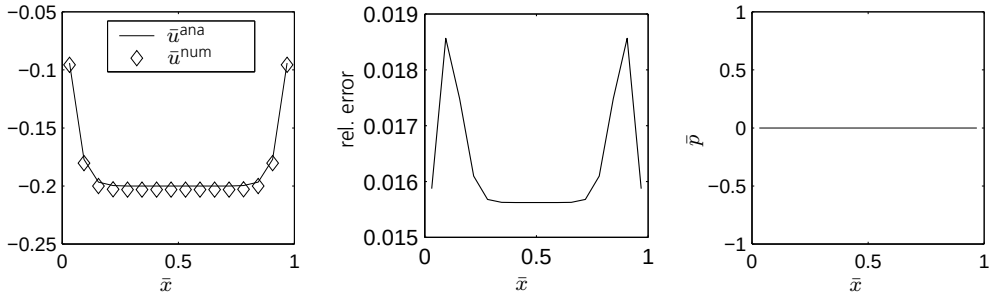

Figure 7 Numerical velocity $\bar{u}^{\text{num}}$ and analytical velocity $\bar{u}^{\text{ana}}$ (left), relative error $\left\|\bar{\boldsymbol{u}} - \boldsymbol{u}^{\bar{\text{num}}}\right\|_2 / \|\bar{\boldsymbol{u}}\|_2$ (middle), as well as numerical pressure $\bar{p}$ (right) for $\bar{t} = 0.2$, $\varphi = 8.0$, and $\Delta x = 1/16$

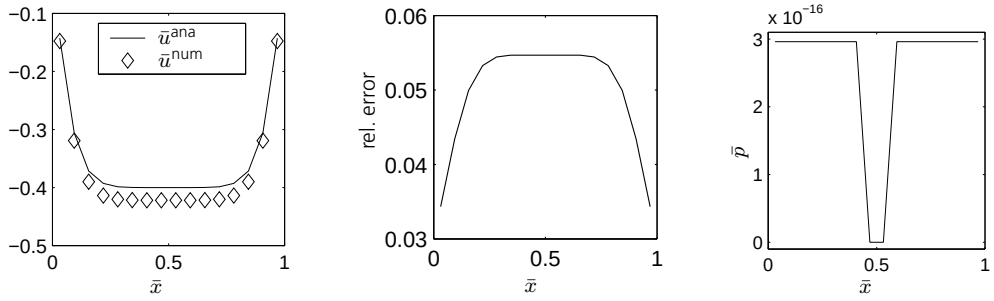

Figure 8 Numerical velocity $\bar{u}^{\text{num}}$ and analytical velocity $\bar{u}^{\text{ana}}$ (left), relative error $\left\|\bar{\boldsymbol{u}} - \boldsymbol{u}^{\bar{\text{num}}}\right\|_2 / \|\bar{\boldsymbol{u}}\|_2$ (middle), as well as numerical pressure $\bar{p}$ (right) for $\bar{t} = 0.4$, $\varphi = 8.0$, and $\Delta x = 1/16$

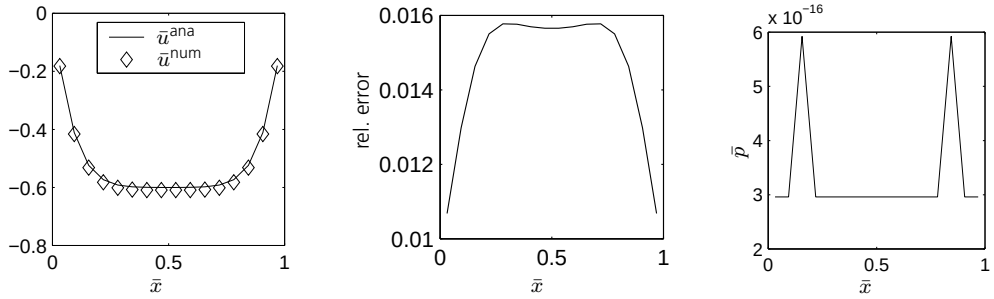

Figure 9 Numerical velocity $\bar{u}^{\text{num}}$ and analytical velocity $\bar{u}^{\text{ana}}$ (left), relative error $\left\|\bar{\boldsymbol{u}} - \boldsymbol{u}^{\bar{\text{num}}}\right\|_2 / \|\bar{\boldsymbol{u}}\|_2$ (middle), as well as numerical pressure $\bar{p}$ (right) for $\bar{t} = 0.6$, $\varphi = 8.0$, and $\Delta x = 1/16$

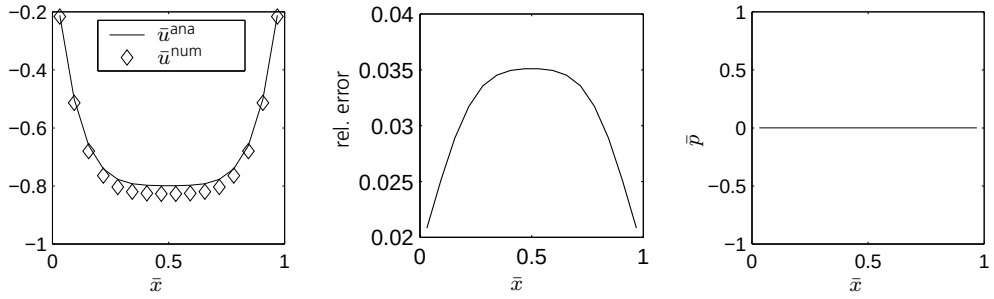

Figure 10 Numerical velocity $\bar{u}^{\text{num}}$ and analytical velocity $\bar{u}^{\text{ana}}$ (left), relative error $\left\|\bar{\boldsymbol{u}} - \boldsymbol{u}^{\bar{\text{num}}}\right\|_2 / \|\bar{\boldsymbol{u}}\|_2$ (middle), as well as numerical pressure $\bar{p}$ (right) for $\bar{t} = 0.8$, $\varphi = 8.0$, and $\Delta x = 1/16$

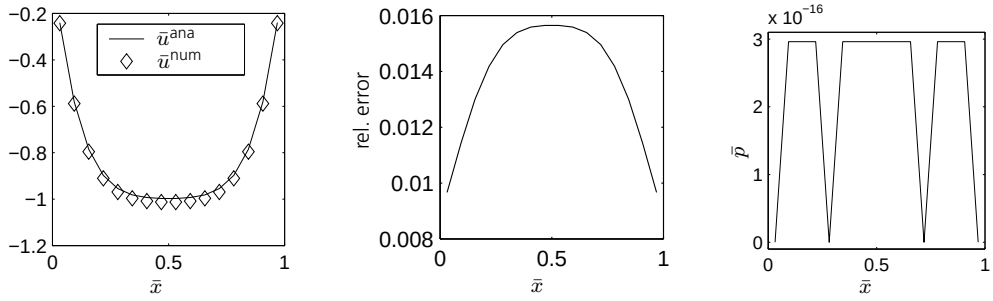

Figure 11 Numerical velocity $\bar{u}^{\text{num}}$ and analytical velocity $\bar{u}^{\text{ana}}$ (left), relative error $\left\|\bar{\boldsymbol{u}} - \boldsymbol{u}^{\bar{\text{num}}}\right\|_2 / \|\bar{\boldsymbol{u}}\|_2$ (middle), as well as numerical pressure $\bar{p}$ (right) for $\bar{t} = 1.0$, $\varphi = 8.0$, and $\Delta x = 1/16$

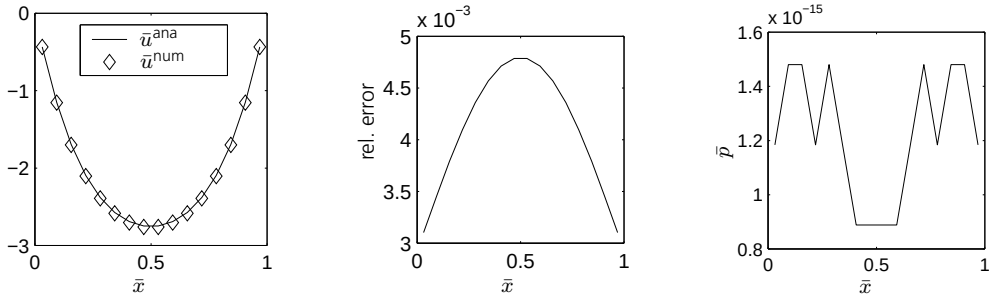

Figure 12 Numerical velocity $\bar{u}^{\text{num}}$ and analytical velocity $\bar{u}^{\text{ana}}$ (left), relative error $\left\|\bar{\boldsymbol{u}} - \boldsymbol{u}^{\bar{\text{num}}}\right\|_2 / \|\bar{\boldsymbol{u}}\|_2$ (middle), as well as numerical pressure $\bar{p}$ (right) for $\bar{t} = 3.0$, $\varphi = 8.0$, and $\Delta x = 1/16$

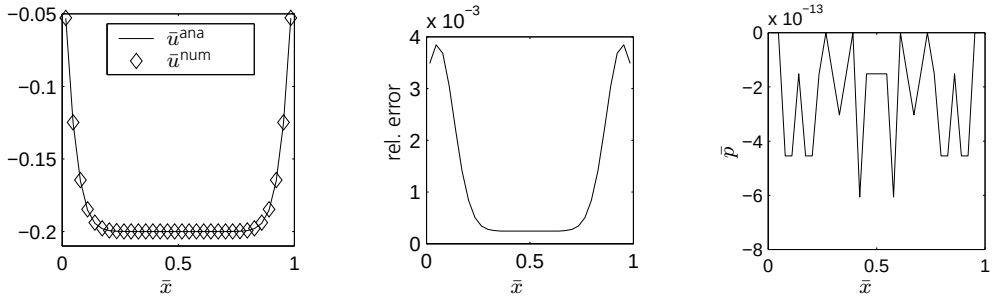

Figure 13 Numerical velocity $\bar{u}^{\text{num}}$ and analytical velocity $\bar{u}^{\text{ana}}$ (left), relative error $\left\|\bar{\boldsymbol{u}} - \boldsymbol{u}^{\bar{\text{num}}}\right\|_2 / \|\bar{\boldsymbol{u}}\|_2$ (middle), as well as numerical pressure $\bar{p}$ (right) for $\bar{t} = 0.2$, $\varphi = 0.5$, and $\Delta x = 1/32$

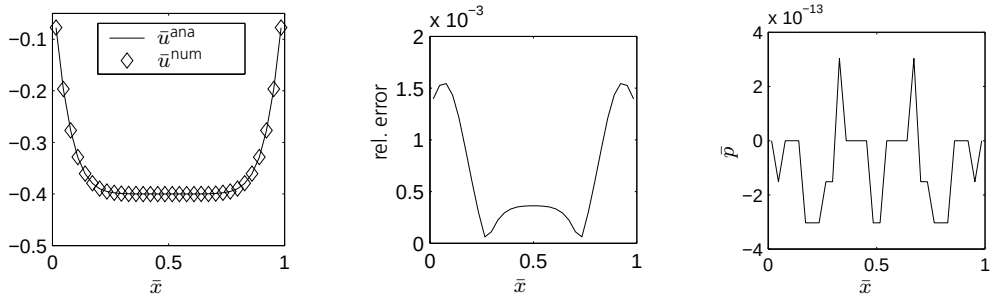

Figure 14 Numerical velocity $\bar{u}^{\text{num}}$ and analytical velocity $\bar{u}^{\text{ana}}$ (left), relative error $\left\|\bar{\boldsymbol{u}} - \boldsymbol{u}^{\bar{\text{num}}}\right\|_2 / \|\bar{\boldsymbol{u}}\|_2$ (middle), as well as numerical pressure $\bar{p}$ (right) for $\bar{t} = 0.4$, $\varphi = 0.5$, and $\Delta x = 1/32$

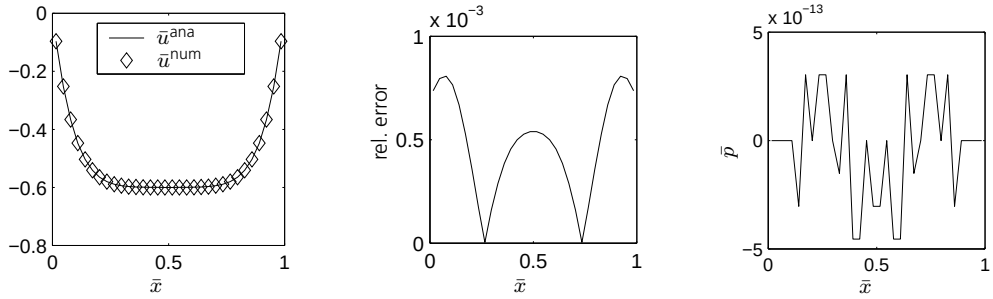

Figure 15 Numerical velocity $\bar{u}^{\text{num}}$ and analytical velocity $\bar{u}^{\text{ana}}$ (left), relative error $\left\|\bar{\boldsymbol{u}} - \boldsymbol{u}^{\bar{\text{num}}}\right\|_2 / \|\bar{\boldsymbol{u}}\|_2$ (middle), as well as numerical pressure $\bar{p}$ (right) for $\bar{t} = 0.6$, $\varphi = 0.5$, and $\Delta x = 1/32$

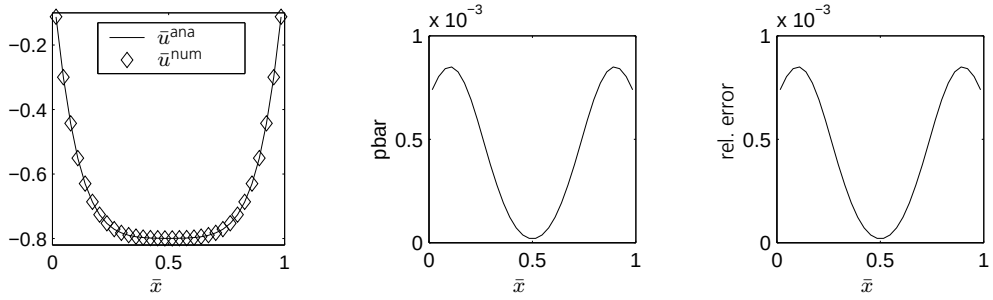

Figure 16 Numerical velocity $\bar{u}^{\text{num}}$ and analytical velocity $\bar{u}^{\text{ana}}$ (left), relative error $\left\|\bar{\boldsymbol{u}} - \boldsymbol{u}^{\bar{\text{num}}}\right\|_2 / \|\bar{\boldsymbol{u}}\|_2$ (middle), as well as numerical pressure $\bar{p}$ (right) for $\bar{t} = 0.8$, $\varphi = 0.5$, and $\Delta x = 1/32$

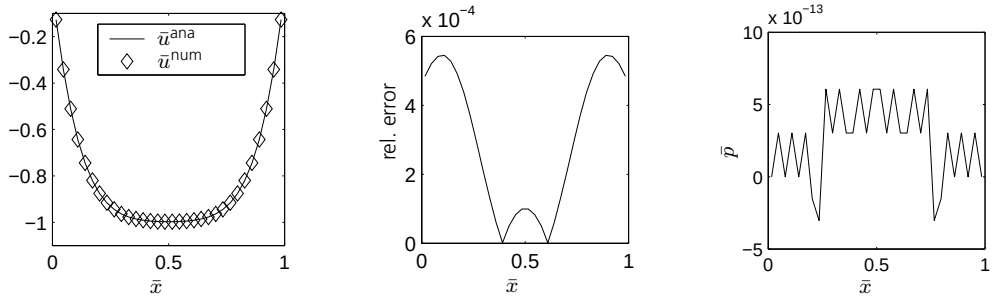

Figure 17 Numerical velocity $\bar{u}^{\text{num}}$ and analytical velocity $\bar{u}^{\text{ana}}$ (left), relative error $\left\|\bar{\boldsymbol{u}} - \boldsymbol{u}^{\bar{\text{num}}}\right\|_2 / \|\bar{\boldsymbol{u}}\|_2$ (middle), as well as numerical pressure $\bar{p}$ (right) for $\bar{t} = 1.0$, $\varphi = 0.5$, and $\Delta x = 1/32$

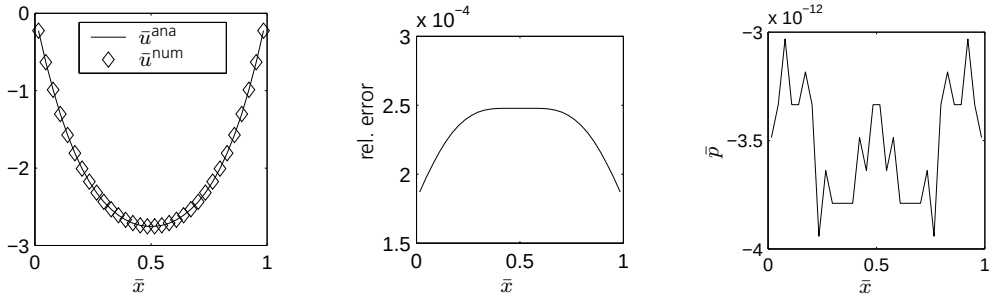

Figure 18 Numerical velocity $\bar{u}^{\text{num}}$ and analytical velocity $\bar{u}^{\text{ana}}$ (left), relative error $\left\|\bar{\boldsymbol{u}} - \boldsymbol{u}^{\bar{\text{num}}}\right\|_2 / \|\bar{\boldsymbol{u}}\|_2$ (middle), as well as numerical pressure $\bar{p}$ (right) for $\bar{t} = 3.0$, $\varphi = 0.5$, and $\Delta x = 1/32$

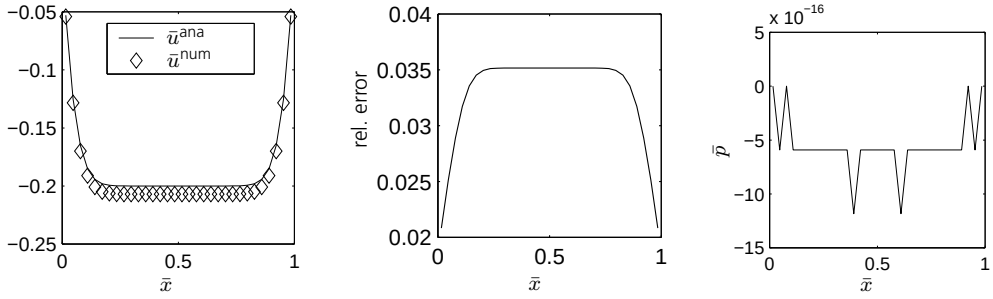

Figure 19 Numerical velocity $\bar{u}^{\text{num}}$ and analytical velocity $\bar{u}^{\text{ana}}$ (left), relative error $\left\|\bar{\boldsymbol{u}} - \boldsymbol{u}^{\bar{\text{num}}}\right\|_2 / \|\bar{\boldsymbol{u}}\|_2$ (middle), as well as numerical pressure $\bar{p}$ (right) for $\bar{t} = 0.2$, $\varphi = 8.0$, and $\Delta x = 1/32$

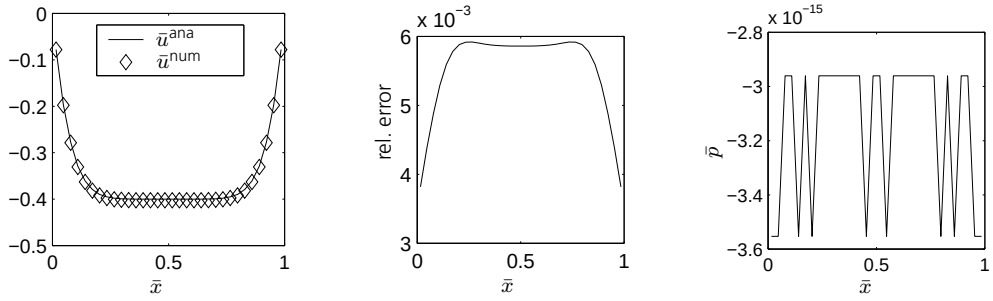

Figure 20 Numerical velocity $\bar{u}^{\text{num}}$ and analytical velocity $\bar{u}^{\text{ana}}$ (left), relative error $\left\|\bar{\boldsymbol{u}} - \boldsymbol{u}^{\bar{\text{num}}}\right\|_2 / \|\bar{\boldsymbol{u}}\|_2$ (middle), as well as numerical pressure $\bar{p}$ (right) for $\bar{t} = 0.4$, $\varphi = 8.0$, and $\Delta x = 1/32$

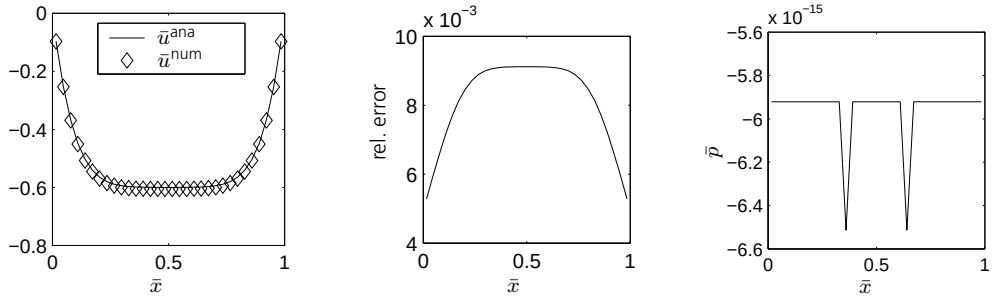

Figure 21 Numerical velocity $\bar{u}^{\text{num}}$ and analytical velocity $\bar{u}^{\text{ana}}$ (left), relative error $\left\|\bar{\boldsymbol{u}} - \boldsymbol{u}^{\bar{\text{num}}}\right\|_2 / \|\bar{\boldsymbol{u}}\|_2$ (middle), as well as numerical pressure $\bar{p}$ (right) for $\bar{t} = 0.6$, $\varphi = 8.0$, and $\Delta x = 1/32$

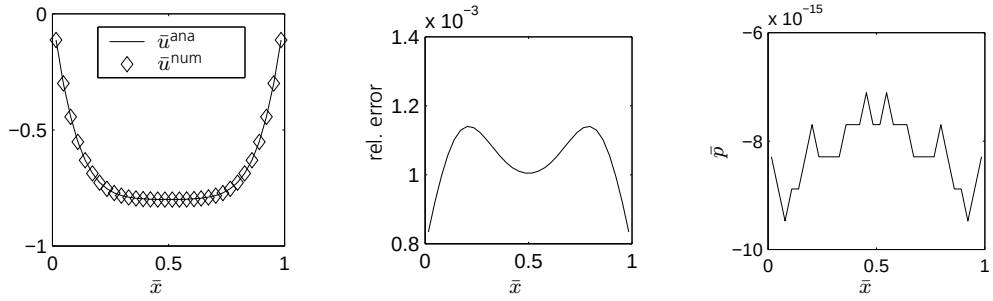

Figure 22 Numerical velocity $\bar{u}^{\text{num}}$ and analytical velocity $\bar{u}^{\text{ana}}$ (left), relative error $\left\|\bar{\boldsymbol{u}} - \boldsymbol{u}^{\bar{\text{num}}}\right\|_2 / \|\bar{\boldsymbol{u}}\|_2$ (middle), as well as numerical pressure $\bar{p}$ (right) for $\bar{t} = 0.8$, $\varphi = 8.0$, and $\Delta x = 1/32$

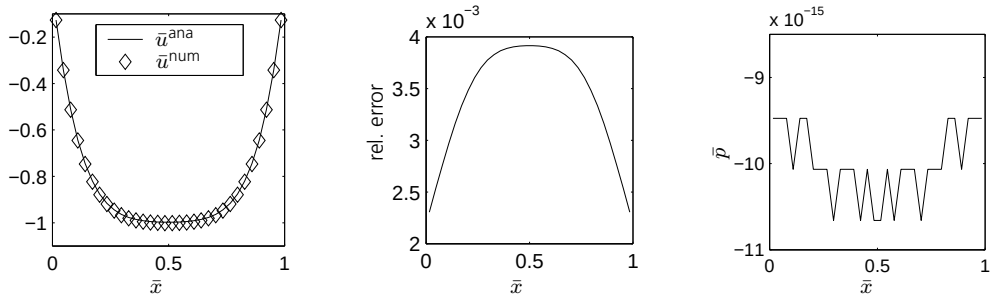

Figure 23 Numerical velocity $\bar{u}^{\text{num}}$ and analytical velocity $\bar{u}^{\text{ana}}$ (left), relative error $\left\|\bar{\boldsymbol{u}} - \boldsymbol{u}^{\text{num}}\right\|_2 / \|\bar{\boldsymbol{u}}\|_2$ (middle), as well as numerical pressure $\bar{p}$ (right) for $\bar{t} = 1.0$, $\varphi = 8.0$, and $\Delta x = 1/32$

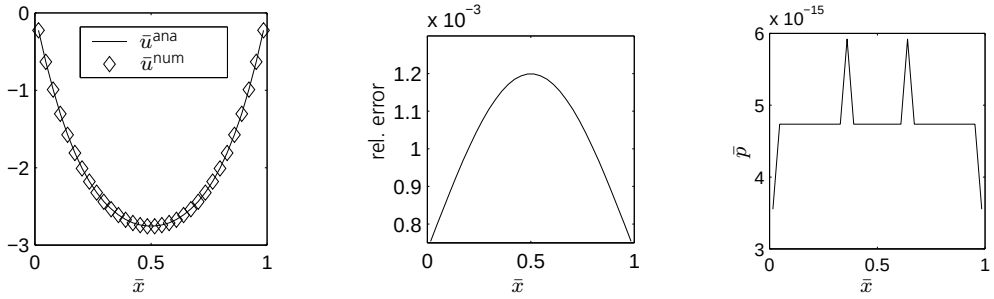

Figure 24 Numerical velocity $\bar{u}^{\text{num}}$ and analytical velocity $\bar{u}^{\text{ana}}$ (left), relative error $\left\|\bar{\boldsymbol{u}} - \boldsymbol{u}^{\text{num}}\right\|_2 / \|\bar{\boldsymbol{u}}\|_2$ (middle), as well as numerical pressure $\bar{p}$ (right) for $\bar{t} = 3.0$, $\varphi = 8.0$, and $\Delta x = 1/32$

References

[1] M. JUNK, A. KLAR, L.-S. LUO, *Asymptotic analysis of the lattice Boltzmann equation,* J. Comput. Phys. **210** (2005), pp. 676-704. 5

[2] M. B. REIDER, J. D. STERLING, *Accuracy of discrete-velocity BGK models for the simulation of the incompressible Navier-Stokes equations,* Computers & Fluids **24** (1995), pp. 459-467. 6